Simulation of an Industrial Nylon 6 Tubular Reactor

SANTOSH K. GUPTA* and MAHARI TJAHJADI, *Department of Chemical Engineering, University of Notre Dame, Notre Dame, Indiana 46556*

Synopsis

A commonly used energy-efficient nylon 6 reactor is simulated under steady-state conditions. The effects of various operating conditions and parameters, e.g., feed composition, temperature and flow rate, heat transfer coefficients, and reactor dimensions, on the temperature and molecular weight profiles are studied. A temperature maximum is observed in the reactor under usual conditions of operation. The maximum value of the temperature is sensitive to the feed conditions, and one has to ensure that degradation reactions speeded up at high temperatures do not affect product characteristics. The model and the numerical technique used are fairly simple and account for most of the important features of industrial reactors. Hence, these can be used in the development of digital-control algorithms in the future.

INTRODUCTION

The manufacture of nylon 6 by the hydrolytic polymerization of ϵ-caprolactam is an important industrial process. Sittig[1] has described several reactor configurations that are being used industrially to produce this polymer. They range from simple batch reactors operating under high pressures (to avoid vaporization) to cascades of stirred tank reactors in combination with tubular reactors. A considerable amount of research has been reported in the last three decades on the modeling of nylon 6 reactors and has formed the basis of several reviews.[2-5] Most of the earlier studies focused attention on isothermal reactors with no vaporization of water and other low-molecular-weight compounds and have helped to establish values for the rate and equilibrium constants for the different main and side reactions. In the last several years, however, researchers in this area have turned their attention to the simulation and optimization of industrial nylon 6 reactors, considering such physical phenomena as heat and mass transfer. This study is in line with this direction and models one kind of a continuous tubular nylon 6 reactor.

The reactor configuration being modeled in this paper is shown schematically in Figure 1. It consists of a jacketed reactor about a meter in diameter containing a coiled tube AB having a radius of a few centimeters. The feed to the reactor, consisting of ϵ-caprolactam (C_1), water (W), acetic acid (A_1) stabilizer, and some inert materials, enters at point A and is preheated to a

*On leave from the Indian Institute of Technology, Kanpur, India

Journal of Applied Polymer Science, Vol. 33, 933–954 (1987)

CCC 0021-8995/87/030933-22$04.00

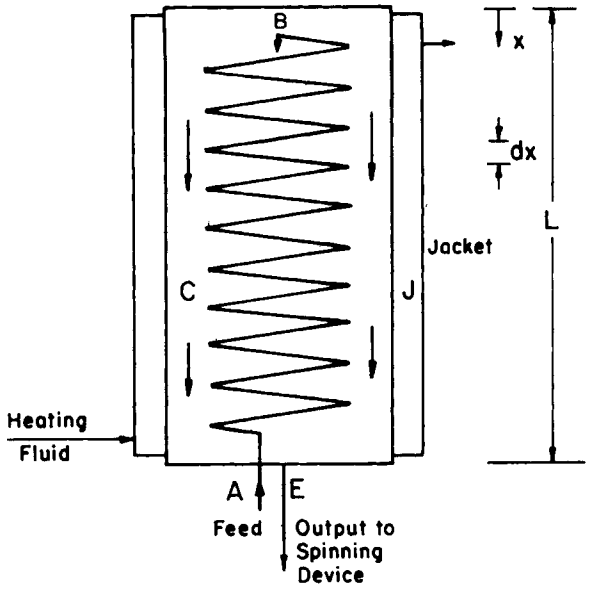

Fig. 1. The reactor configuration.

temperature in the range of 220–240°C as it flows up inside the coiled tube. At point B, the reaction mass leaves the coiled tube and flows down over the coil inside the jacketed column. Thus, the reactor could be described in terms of two regions of flow—the tube, referred to by subscript t later, and the region outside the tube (hereafter called column), denoted by subscript c. There is no exchange of mass between these two regions, except at point B in Figure 1. As the reaction mass moves down slowly inside the column, it exchanges heat with both the fluid in the jacket (J), and the material inside the tube. The major part of the polymerization takes place here, and the number-average chain length (or degree of polymerization) μ_n increases to the desired value by the time the reaction mass reaches the exit (E) of the reactor. The values of μ_n and other properties of the product stream depend on the feed conditions as well as on the temperature profiles in the tube and the column. The pressure inside the reactor is maintained high enough at all locations to suppress the vaporization of low-molecular-weight compounds. Such a reactor has the advantage of being energy efficient since part of the heat of reaction is utilized for preheating the feed in the same piece of equipment. However, the heat integration makes this reactor more sensitive to minor variations in the input variables (disturbances) and explains why this design is not as popular as it should be these days when energy is expensive and the competition for lower production costs is intense. With the advent of inexpensive process-control computers, it is possible to develop advanced control algorithms for this reactor that will help overcome its inherent problems of sensitivity and thus make it an attractive design. The techniques developed in this continuing program of study, although illustrated for nylon 6 systems, are far more general and can be used for other tubular polymerization reactors.

The first step in the design of a control algorithm for reactors of the type shown in Figure 1 is the development of a steady-state model. This is the focus of the present work. Dynamic models for this reactor are being developed and will be discussed in future publications, along with designs of feasible computer-control algorithms.

At the very outset, it must be emphasized that, for the design of controllers, the model for the reactor must be fairly simple so that it explains only its gross physical behavior. Less important second-order effects need not be considered since they can be taken care of by the digital computer control algorithm (adaptation). The model for this reactor differs significantly from that of VK columns.[6-8] Since there is no vaporization in this reactor, the difficulties associated with modeling the mixing effects caused by the rise of vapor bubbles in the VK column are absent. Also, vapor-liquid equilibrium relationships are not necessary. Heat transfer effects assume much greater significance than in the VK column; the latter have usually been modeled as sequences of *isothermal* continuous-flow stirred-tank reactors (CSTR) followed by isothermal or adiabatic plug flow reactors. Because of the countercurrent flow existing in the two regions of the reactor (tube and column), more complex numerical techniques are required to solve the set of ordinary differential equations describing this reactor.

FORMULATION

Model for the Reactor

The kinetic scheme used in this work is given in Table I, along with the rate and equilibrium constants. The bifunctional (S_n) and monofunctional (A_n) molecular species present in the reaction mass, as well as the cyclic oligomers (C_n) present, are defined in Table I. This represents the most recent and precise data on nylon 6 polymerization available in the literature[9-14] and is now used in most simulation[13,15-18] and optimization[19-22] studies. The rate and equilibrium constants for the first three reactions differ slightly from the earlier values of Reimschuessel.[2] Table I incorporates the three major reactions, ring opening, polycondensation, and polyaddition, as well as reactions involving the monofunctional acid stabilizers and the cyclic dimer. The reactions with higher cyclic oligomers are not incorporated in this scheme since equally precise rate constants are not yet available. Recently there has been a study[14] that presents experimental data on the buildup of the various cyclic oligomers with time, but this has not yet been curve fitted to give the rate constants because of mathematical difficulties. However, since the cyclic dimer constitutes the major share of the total cyclic oligomers, very little error is expected because of this approximation. Incorporating the various reactions in the kinetic scheme gives a more detailed description of reactor behavior and also provides a better means of confirming or fine tuning the theoretical model if appropriate data (e.g., temperature profile, $[C_1]$, $[C_2]$, and number- and weight-average molecular weights of the product) are available on actual reactors or pilot plants under different operating conditions. Fur-

TABLE I
Kinetic Scheme for Nylon 6 Polymerization[a]

1. Ring opening:

$$C_1 + W \underset{k_1' = k_1/K_1}{\overset{k_1}{\rightleftharpoons}} S_1$$

2. Polycondensation:

$$S_n + S_m \underset{k_2' = k_2/K_2}{\overset{k_2}{\rightleftharpoons}} S_{n+m} + W$$

3. Polyaddition:

$$S_n + C_1 \underset{k_3' = k_3/K_3}{\overset{k_3}{\rightleftharpoons}} S_{n+1}$$

4. Reaction with monofunctional acid:

$$S_n + A_m \underset{k_2'}{\overset{k_2}{\rightleftharpoons}} A_{n+m} + W$$

5. Ring opening of cyclic dimer:

$$C_2 + W \underset{k_4' = k_4/K_4}{\overset{k_4}{\rightleftharpoons}} S_2$$

6. Polyaddition of cyclic dimer:

$$S_n + C_2 \underset{k_5' = k_5/K_5}{\overset{k_5}{\rightleftharpoons}} S_{n+2}$$

Rate and equilibrium constants

$$k_i = A_i^0 e^{(-E_i^0/RT)} + A_i^c e^{(-E_i^c/RT)} \sum_{n=1}^{\infty} ([A_n] + [S_n])$$

$$\equiv k_i^0 + k_i^c \sum_{n=1}^{\infty} ([S_n] + [A_n])$$

$$K_i = e^{(\Delta S_i - \Delta H_i/T)/R} \qquad i = 1, 2, \ldots, 5$$

i	A_i^0 (kg/mol-h)	E_i^0 (cal/mol)	A_i^c (kg^2/mol^2-h)	E_i^c (cal/mol)	ΔH_i (cal/mol)	ΔS_i (eu)
1	5.9874×10^5	1.9880×10^4	4.3075×10^7	1.8806×10^4	1.9180×10^3	-7.8846×10^0
2	1.8942×10^{10}	2.3271×10^4	1.2114×10^{10}	2.0670×10^4	-5.9458×10^3	9.4374×10^{-1}
3	2.8558×10^9	2.2845×10^4	1.6377×10^{10}	2.0107×10^4	-4.0438×10^3	-6.9457×10^0
4	8.5778×10^{11}	4.2000×10^4	2.3307×10^{12}	3.7400×10^4	-9.6000×10^3	-1.4520×10^1
5	2.5701×10^8	2.1300×10^4	3.0110×10^9	2.0400×10^4	-3.1691×10^3	5.8265×10^{-1}

[a] C_1: ε-caprolactam; C_n: H—N—$(CH_2)_5$—C(=O)—N—$(CH_2)_5$—C(=O)$_n$; W: water; S_n: H—[N—$(CH_2)_5$—C(=O)]$_n$—OH; A_n: X[C(=O)—N—$(CH_2)_5$]$_{n-1}$C(=O)—OH, X unreactive group; T = temperature; R = gas constant.

TABLE II
Balance Equations for Tube and Column

Tube t equations:

$$\frac{d}{dx}(\rho V_t) = 0$$

$$-\frac{d}{dx}(\rho V_t \xi_i) = \rho S \dot{\xi}_i \qquad i = 1, 2, \ldots, 10$$

where $\xi = [C_1], [S_1], \mu_0, \mu_1, \mu_2, [C_2], [W], \mu_1', \mu_2', [A_1]$

$$\frac{d}{dx}(\rho V_t C_p T_t) = \frac{2U_t}{r_t} S(T_t - T_c) - \rho S \sum_{i=1}^{6} \frac{(-\Delta H_{r,i})}{10^3} \mathscr{R}_i$$

Column c equations:

$$\frac{d}{dx}(\rho V_c) = 0$$

$$\frac{d}{dx}(\rho V_c \xi_i) = \rho \dot{\xi}_i \qquad \xi_i \text{ as above, } i = 1, 2, \ldots, 10$$

$$\frac{d}{dx}(\rho V_c C_p T_c) = \frac{2r_t S}{r_c^2} U_t (T_t - T_c) + \frac{2U_J}{r_c}(T_J - T_c) + \rho \sum_{i=1}^{6} \frac{(-\Delta H_{r,i})}{10^3} \mathscr{R}_i$$

Continuity between t and c (at $x = 0$):

$$V_t A_t = V_c A_c$$

$$\xi_{i,t} = \xi_{i,c} \qquad i = 1, 2, \ldots, 10$$

$$T_t = T_c$$

Property correlations:

$$\rho = \frac{1000}{1.0065 + 0.0123[C_1] + (T - 495)(0.00035 + 0.00007[C_1])}$$

$$C_p = 0.6593 \frac{[C_1]}{[C_1]_0} + \left(1 - \frac{[C_1]}{[C_1]_0}\right)(0.4861 + 0.000337T)$$

thermore, any simulation study must give a good estimate of the cyclic oligomer content in the product, since these compounds create problems in spinning and are usually removed by leaching with hot water, a highly energy intensive process.

Mass and energy balance equations for steady-state operation, for both the tube and the column sides, are given in Table II, along with the continuity

equation at point B of Figure 1 (see Nomenclature for units and definitions of the variables used). This table also includes balance equations for the moments

$$\mu_k \left(\equiv \sum_{n=1}^{\infty} n^k [S_n] \right)$$

and

$$\mu'_k \left(\equiv \sum_{n=1}^{\infty} n^k [A_n] \right)$$

of the chain length distributions of the bifunctional and monofunctional molecular species. The equations in Table II assume plug flow and neglect radial temperature variations on both the tube and column sides. The former is a fairly good approximation since the presence of column internals usually leads to an almost flat velocity profile. Neglecting the radial gradients may not be entirely justified and is done purely to keep the model simple. Incorporating radial temperature gradients in the column being considered here will necessitate the use of finite-element techniques[23] for solution and may, in fact, be necessary if the objective is to have an excellent model for this reactor. However, the goal of our program of study is to develop models that can be used in the future for designing digital adaptive controllers. Because of some amount of mixing induced by the column internals, it is believed that the radial gradients will be dampened out somewhat, and our model should be fairly good.

Changes in the density ρ (and so the velocity) and the specific heat C_p associated with the changes in temperature and the concentrations with position are allowed for. Correlations for the physical properties of the reaction mass are those suggested by Jacobs and Schweigman[6] and are used in our study since they are more general than the more recent correlations of Tai et al.[18] Since the values of ρ and C_p, as obtained from Table II, differ by about 10% from those computed using the correlations of Tai et al., it is necessary to carry out a sensitivity study to see if the use of different correlations leads to significantly different predictions for reactor performance.

Table II requires equations for the rate of generation $\dot{\xi}$, by chemical reaction, of the various species and moments, as well as equations for the net forward rate $\mathscr{R}_i$, associated with each of the six reactions in Table I. These are given[15] in Table III. These equations are similar to those of Tai et al.[9-11] and are also consistent with those given by Hermans et al.,[24] Hoftyzer et al.,[25] and Reimschuessel.[2] Closure conditions are required to break the hierarchy of equations, and Table III incorporates appropriate equations for this purpose. These simple closure conditions have been demonstrated[4,5,9,17,26] to give correct results[27,28] for the first three moments for several types of nylon 6 reactors operating under an extremely wide range of operating conditions and

TABLE III
Equations for ξ and $\mathscr{R}_i$ of Table II and Closure Conditions

$$[\dot{C}_1] = -k_1[C_1][W] + k_1'[S_1] - k_3[C_1]\mu_0 + k_3'(\mu_0 - [S_1])$$

$$[\dot{S}_1] = k_1[C_1][W] - k_1'[S_1] - 2k_2[S_1]\mu_0 + 2k_2'[W](\mu_0 - [S_1]) - k_3[S_1][C_1]$$
$$+k_3'[S_2] - k_2\mu_0'[S_1] + k_2'[W](\mu_0' - [A_1]) - k_5[S_1][C_2] + k_5'[S_3]$$

$$\dot{\mu}_0 = k_1[C_1][W] - k_1'[S_1] - k_2\mu_0^2 + k_2'[W](\mu_1 - \mu_0) - k_2\mu_0\mu_0' + k_2'[W](\mu_1' - \mu_0')$$
$$+k_4[W][C_2] - k_4'[S_2]$$

$$\dot{\mu}_1 = k_1[C_1][W] - k_1'[S_1] + k_3[C_1]\mu_0 - k_3'(\mu_0 - [S_1]) - k_2\mu_0'\mu_1 - \tfrac{1}{2}k_2'[W](\mu_1' - \mu_2')$$
$$+2k_5[C_2]\mu_0 - 2k_5'(\mu_0 - [S_1] - [S_2]) + 2k_4[W][C_2] - 2k_4'[S_2]$$

$$\dot{\mu}_2 = k_1[C_1][W] - k_1'[S_1] + 2k_2\mu_1^2 + \tfrac{1}{3}k_2'[W](\mu_1 - \mu_3) + k_3[C_1](\mu_0 + 2\mu_1)$$
$$+k_3'(\mu_0 - 2\mu_1 + [S_1]) - k_2\mu_2\mu_0' + \tfrac{1}{6}k_2'[W](2\mu_3' - 3\mu_2' + \mu_1') + 4k_5[C_2](\mu_1 + \mu_0)$$
$$+4k_5'(\mu_0 - \mu_1 + [S_2]) + 4k_4[W][C_2] - 4k_4'[S_2]$$

$$[\dot{C}_2] = -k_4[C_2][W] + k_4'[S_2] - k_5[C_2]\mu_0 + k_5'(\mu_0 - [S_1] - [S_2])$$

$$[\dot{W}] = -k_1[C_1][W] + k_1'[S_1] + k_2(\mu_0)^2 - k_2'[W](\mu_1 - \mu_0) + k_2\mu_0\mu_0' - k_2'[W](\mu_1' - \mu_0')$$
$$-k_4[C_2][W] + k_4'[S_2]$$

$$\dot{\mu}_1' = k_2\mu_1\mu_0' - \tfrac{1}{2}k_2'[W](\mu_2' - \mu_1')$$

$$\dot{\mu}_2' = k_2(2\mu_1\mu_1' + \mu_2\mu_0') - \tfrac{1}{6}k_2'[W](4\mu_3' - 3\mu_2' - \mu_1')$$

$$[\dot{A}_1] = -k_2[A_1]\mu_0 + k_2'[W](\mu_0' - [A_1])$$

$$\dot{\mu}_0' = 0, \text{ or } \mu_0' = \text{constant } (= \text{inlet value})$$

$$\mathscr{R}_1 = k_1[C_1][W] - k_1'[S_1]$$

$$\mathscr{R}_2 = k_2\mu_0^2 - k_2'[W](\mu_1 - \mu_0)$$

$$\mathscr{R}_3 = k_3[C_1]\mu_0 - k_3'(\mu_0 - [S_1])$$

$$\mathscr{R}_4 = k_2\mu_0\mu_0' - k_2'[W](\mu_1' - \mu_0')$$

$$\mathscr{R}_5 = k_4[C_2][W] - k_4'[S_2]$$

$$\mathscr{R}_6 = k_5[C_2]\mu_0 - k_5'(\mu_0 - [S_1] - [S_2])$$

Closure conditions:

$$[S_2] = [S_3] = [S_1]$$

$$\mu_3 = \frac{\mu_2(2\mu_2\mu_0 - \mu_1^2)}{\mu_1\mu_0} \qquad \mu_3' = \frac{\mu_2'(2\mu_2'\mu_0' - \mu_1'^2)}{\mu_1'\mu_0'}$$

are a special case of the more general closure conditions of Hulburt and Katz.[29]

Numerical Technique

The initial conditions for the tube side are known at $x = L$ (point A in Fig. 1) for any simulation work. However, those for the column side are known at $x = 0$. Thus one has a two-point boundary value problem.[23] The simplest numerical technique used to solve such a set of equations is the method of successive substitutions. A (discretized) temperature *profile*, $T_c^{(0)}(x)$, is assumed (usually isothermal), the equations for the tube side are integrated using the fourth-order Runge Kutta method from $x = L$ to $x = 0$, the continuity conditions in Table II are used to obtain the columnside conditions at $x = 0$, and then the columnside equations are integrated from $x = 0$ to $x = L$, also using the fourth-order Runge Kutta method. This comprises one iteration of calculations. The *computed* column temperatures $T_c^{(k+1)}(x)$ in the kth iteration are compared against the *assumed* values $T_c^{(k)}(x)$, $k = 0, 1, 2, \ldots$, and if the convergence criterion $\{|T_c^{(k+1)}(x) - T_c^{(k)}(x)| \leq \epsilon\}$ is met at *all* (discretized) positions, no further computations are required. If not, the values of $T_c^{(k+1)}(x)$ are used in the next iteration. A typical run on a PRIME 9950 took about 100 s of computer time and about 20 iterations for convergence to be attained. The reason this simple numerical technique worked so well for the present problem may be because of the relatively low heat generation effects.

Several checks were made on our computer program to ensure that it was free of error. Simulations under isothermal conditions were carried out, using appropriate IF statements in the program, and the results obtained were compared with our earlier results[21,22] using the reaction time t given by $t = (L - x)S/V_t$ for the tube and $t = LS/V_t + x/V_c$ for the column side. Excellent agreement was obtained for the monomer conversion ($\equiv 1 - [C_1]/[C_1]_0$), number-average chain length, μ_n $\{\equiv (\mu_1 + \mu_1')/(\mu_0 + \mu_0')\}$, polydispersity index (PDI) $\{\equiv (\mu_2 + \mu_2')(\mu_1 + \mu_1')^{-1}/[(\mu_1 + \mu_1')(\mu_0 + \mu_0')^{-1}]\}$, and the cyclic dimer concentration, thus indicating the correctness of the several mass balance equations as well as the logic of the program. The program was then run for adiabatic conditions (i.e., $U_J = U_t = 0$). Unfortunately, no *detailed* published information was available in the literature with which we could compare our results for adiabatic operation of batch or tubular reactors with feed consisting of only monomer and water. We did find, however, that our temperature rise of about 12°C from the time μ_n increased from about 120 to about 185 was similar in magnitude to that found by Tai et al.,[18] who assumed the feed to the tubular reactor to come from a CSTR and also assumed some heat losses because of vaporization prior to the point where their μ_n became 120. Our computer results for adiabatic operation were also close to values obtained by hand calculations for a Δt of about 2 h. Moreover, convergence was attained for *adiabatic* operation in exactly two iterations, as expected, since the tubeside equations are then uncoupled from the columnside equations.

Parameter Values

The following set of conditions, called reference values, has been used to obtain results:

$$
\begin{aligned}
[C_1]_0 &= 8.8 \text{ mol/kg mixture} \\
[W]_0 &= 0.15 \text{ mol/kg mixture} \\
[S_1]_0 &= \mu_{0,0} = \mu_{1,0} = \mu_{2,0} = [C_2]_0 = \mu'_{1,0} = \mu'_{2,0} = [A_1]_0 = 0.0 \\
T_0 &= 488 \text{ K} \\
V_{t,0} &= 200 \text{ m/h} \\
r_t &= 0.025 \text{ m} \\
r_c &= 0.35 \text{ m} \\
L &= 20 \text{ m} \\
S &= 15 \text{ m/m} \\
T_J &= 530 \text{ K} \\
U_t &= 5 \text{ kcal/m}^2\text{-h-K} \\
U_J &= 1 \text{ kcal/m}^2\text{-h-K}
\end{aligned}
\tag{1}
$$

These are typical for a 10–15 tons/day nylon 6 reactor. Detailed sensitivity studies are then carried out by varying one parameter at a time, keeping all others at their reference values, in order to identify the most important variables. The estimate of the overall heat transfer coefficient for the jacket U_J is made by neglecting both the jacketside coefficient (condensing vapor) and the wall resistance and using standard correlations[30] for heat transfer in fully developed laminar flow inside a pipe. Since the Reynolds numbers are extremely low (approximately 0.05–0.3), the value of U_J is independent of the viscosity of the reaction mass flowing in the column. No significant errors are therefore made in estimating U_J because of the lack of good correlations for the viscosity of polymer-caprolactam mixtures. The estimate for the tubeside overall heat transfer coefficient U_t is made by neglecting the metal resistance and using correlations for the heat transfer coefficient for flow inside a *straight* pipe (since coil diameter $\gg$ tube diameter) and for the flow of a liquid across a bank of straight tubes (again, neglecting the effects of coiling). Average values for the physical properties in the tube and column are used for obtaining these estimates, and it is assumed in this first study that U_t (and also U_J) is independent of position. Unfortunately, there is considerable uncertainty in the values of the viscosity of the reaction mass. The value of about 40 P at the end of typical industrial reactors, as reported by Mashelkar,[31] differs significantly from that of about 550 P obtained using the correlations

of Tai et al.[13] under similar conditions. Such discrepancies in estimates of viscosity, particularly at high conversions, are not limited to nylon 6 systems and are common in other systems, too.[5] The best that one can do at the present state of knowledge is to assume U_t as a parameter to curve fit results on pilot plants or industrial reactors. A value of $U_t = 5$ kcal/m^2-h-K is selected for this study since it gives product properties that are typically encountered in industrial reactors. It is found that the results are quite sensitive to the value of U_t and so one must fine-tune this parameter for actual simulation purposes or, if possible, use in-house proprietary correlations for it, preferably with U_t being a function of position.

RESULTS AND DISCUSSION

Figures 2 through 5 show the steady-state profiles of temperature, degree of polymerization, conversion of the monomer, and the cyclic dimer concentration for the reference conditions given in eq. (1). The value of Δx used was 0.05 m, and the guess temperature profile $T_c^{(0)}(x)$ was 245°C. The convergence parameter ϵ was 1 K. To attain convergence, 18 iterations were required. No change in the profiles was observed when Δx was reduced to 0.02 m (although overflow problems arose when Δx was increased to about 0.2 m), or when $T_c^{(0)}(x)$ was taken as 255°C. The latter choice reduced the number of iterations to 13. In fact, one could possibly reduce the number of iterations still further by assuming a slightly higher value of $T_c^{(0)}(x)$, but this was not pursued any further since the computer time required was reasonably small. A

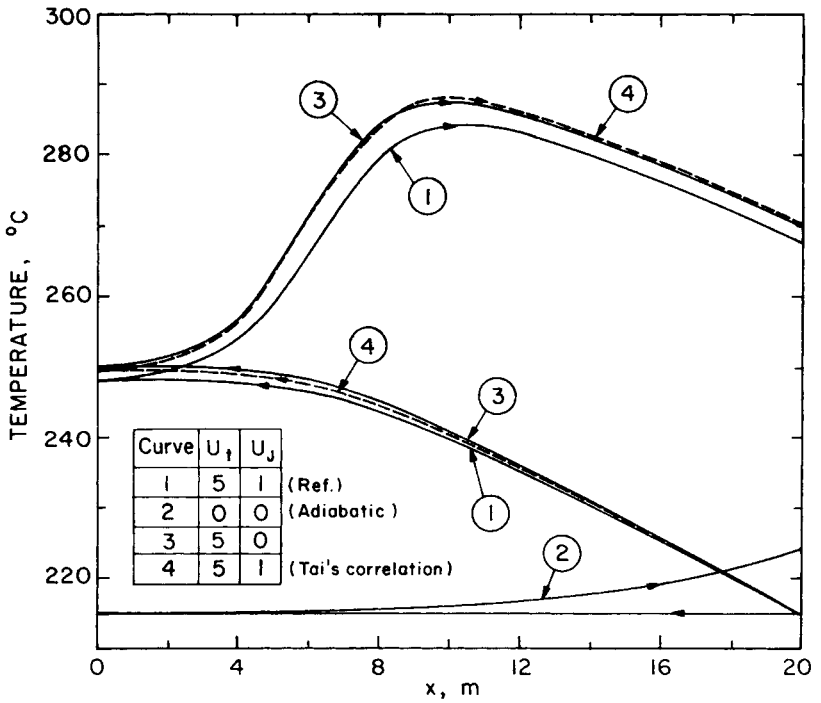

Fig. 2. Temperature profiles for several conditions. Values of parameters not specified are equal to the reference values [eq. (1)].

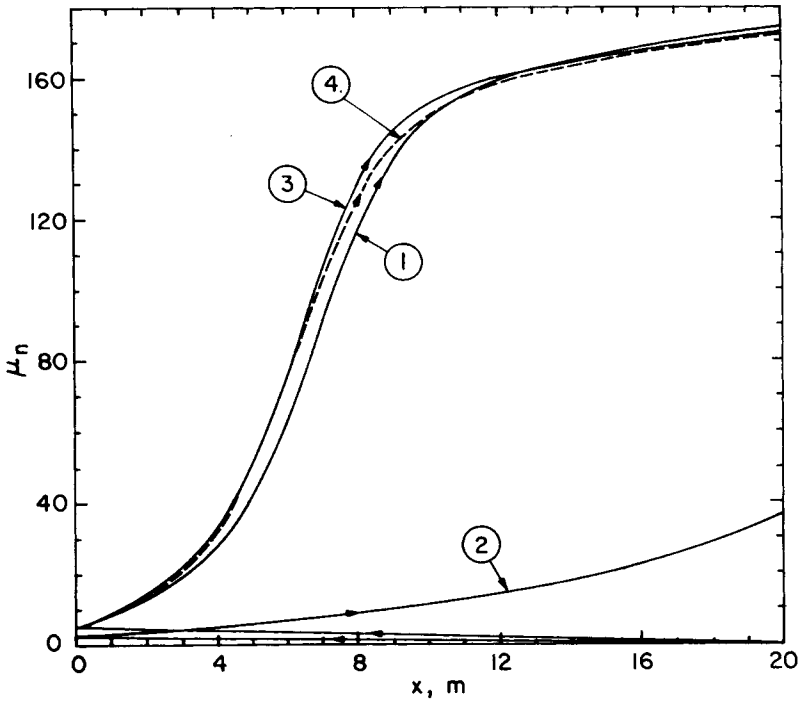

Fig. 3. Profiles for $\mu_n(x)$. Notation as in Figure 2.

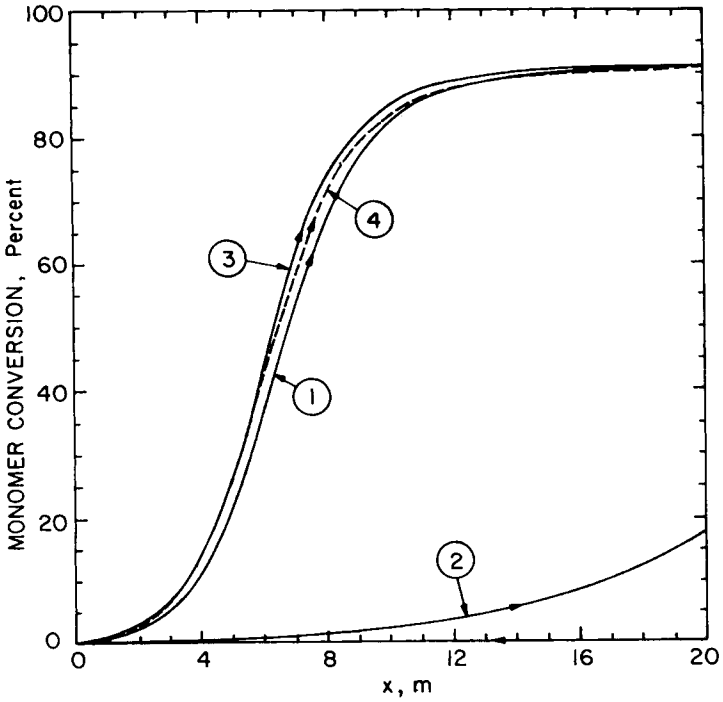

Fig. 4. Monomer conversion as a function of position. Notation as in Figure 2.

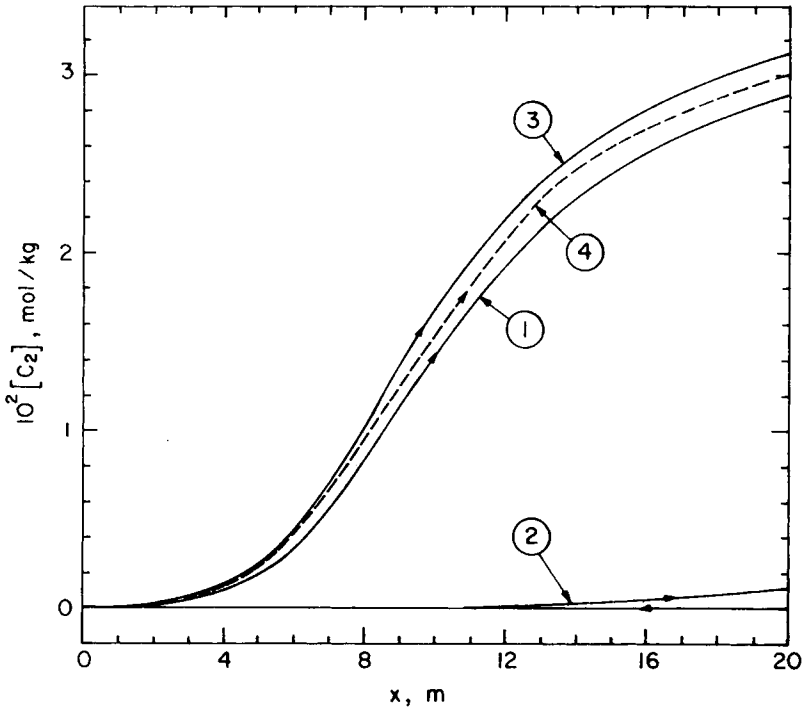

Fig. 5. $[C_2]$ as a function of position for the conditions of Figure 2.

decrease in the computational parameter ϵ to 0.5 K also did not lead to any appreciable changes in the final results, although the number of iterations required for convergence increased.

Figures 2 through 5 show that relatively little polymerization takes place inside the tube, although the temperature of the reaction mass increases by almost 35°C by the time it reaches the column side. Thereafter, there is a sharp increase in the conversion and μ_n, and the temperature goes through a maximum. Near-equilibrium conditions are gradually reached at the end of the reactor. The results shown in these figures show somewhat analogous features to isothermal results in which μ_n shoots up (autoacceleration) as the polycondensation and polyaddition reactions take over from the ring-opening step. It must be re-emphasized that, since the velocities are much lower, the reaction times associated with any Δx in the column side are much larger than corresponding values in the tube. Figures 2 through 5 also show that the results for the reference conditions are quite different from those for adiabatic operation ($U_J = U_t = 0$), demonstrating the necessity of heat exchange to the liquid inside the tube in order to achieve higher conversions and molecular weights.

Figures 2 through 5 also show results with $U_J = 0$ and $U_t = 5$. It is observed that all four *profiles* are slightly different. However, the values of T, μ_n, and monomer conversion at the end of the reactor are almost the same as those obtained for the reference run. The cyclic dimer concentration is higher by about 6% over the reference value of 0.0289 mol/kg. In most cases, then, no significant errors are expected in simulation results because of errors in the

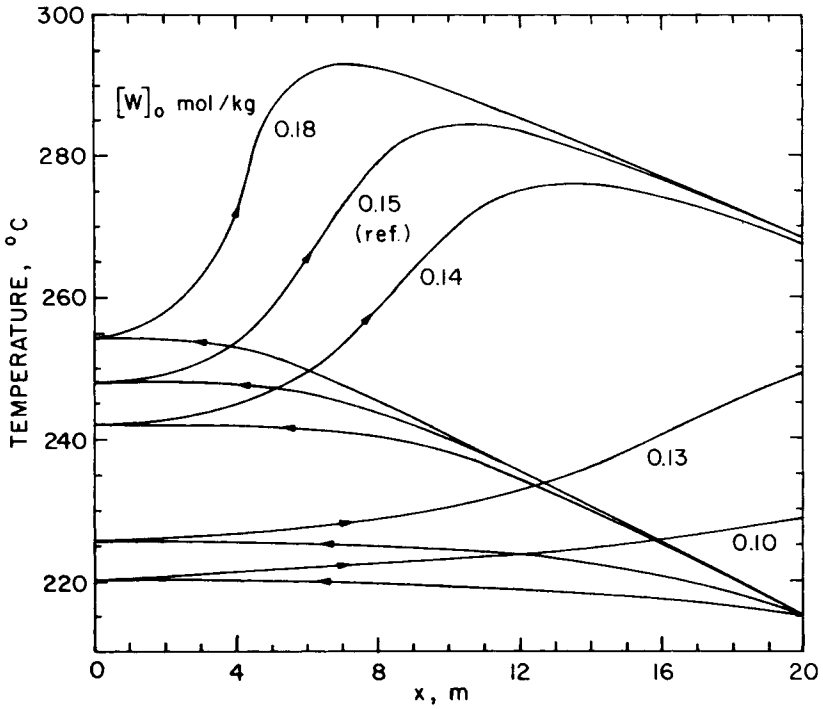

Fig. 6. Effect of the feed water concentration $[W]_0$ on the temperature profile in the reactor.

estimation of U_J. Results obtained using the following correlations of Tai et al.,[13]

$$\rho = 1000\,[1.1238 - 0.000566(T - 273)] \tag{2a}$$

$$C_p = 0.5 + 0.0005(T - 273) \tag{2b}$$

instead of those given in Table II, and with the reference values in eq. (1), are also shown in Figures 2 through 5. The temperature profile is found to be higher by about 2°C almost throughout the column. μ_n and the monomer conversion profiles are also slightly different, although the product values are unaffected. The cyclic dimer concentration is about 3% higher over the reference value. It is interesting to observe that the deviations obtained from the reference values using $U_J = 0$ are of the same order as those obtained using eq. (2). Such differences indicate that the results are not highly sensitive to these two parameters or conditions and one can use any reasonable value for them.

Figures 6 and 7 show the effect of varying the concentration $[W]_0$ of water in the feed with the other variables kept at their reference values. It is found that, for low $[W]_0$, the molecular weights of the nylon 6 are quite low. This is because the ring-opening reaction is sluggish when water concentrations are low. As $[W]_0$ increases, products with higher molecular weights are obtained. However, when $[W]_0$ is increased beyond some value, the equilibrium of the reactions assumes importance, and lower molecular weight products are obtained. The temperature profiles shown in Figure 6 illustrate similar effects.

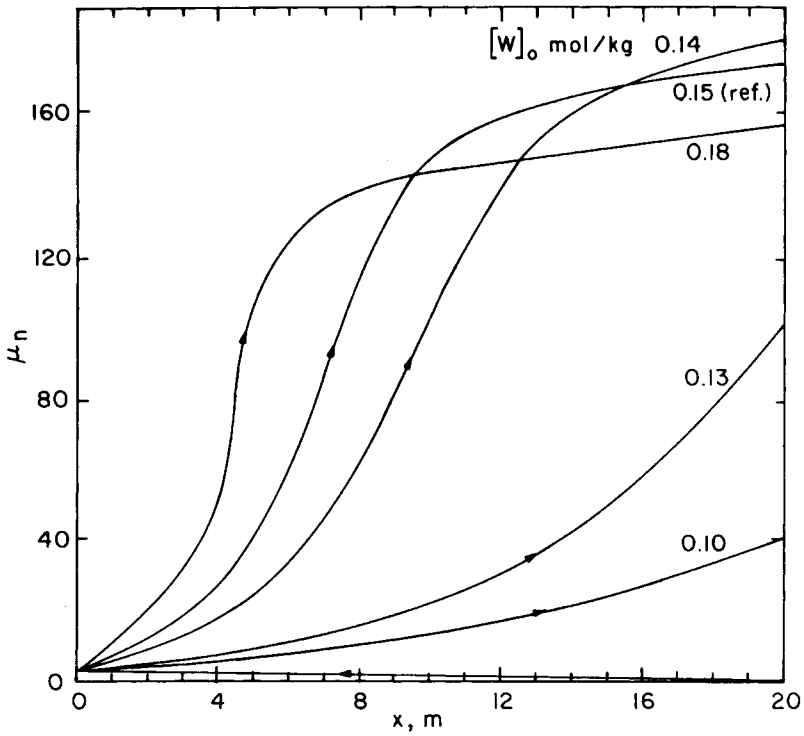

Fig. 7. Effect of $[W]_0$ on the profile of μ_n.

An increase in $[W]_0$ beyond some critical level leads to a peak in the temperature since heat cannot be removed rapidly enough. This may be undesirable from a product property point of view because of degradation reactions.

The possibility of two values of $[W]_0$ giving the same product μ_n is clearly demonstrated in Figure 7 and in Table IV. The lower $[W]_0$ leads to lower values for temperature, $[C_2]$, and monomer conversion. If one is dealing with situations in which the equilibrium conversions obtained with the two values of $[W]_0$ (giving the same product μ_n) differ by only a small percentage, one can easily choose the lower $[W]_0$ and avoid high temperatures. However, if monomer conversions are too low, one is forced to use the higher $[W]_0$, even though it may lead to significantly higher temperature peaks. This figure also suggests the possibility of interesting *dynamic* behavior of the reactor.

Figures 8 and 9 show the sensitivity of the temperature and μ_n profiles to the feed temperature T_0. The reaction is almost quenched when T_0 is below about 211°C. However, an increase in the feed temperature from 211.3 to 211.5°C leads to a significant increase in the exit values of μ_n, monomer conversion, and $[C_2]$ (Table IV; runs 0 and 5–10). Undesirable temperature peaks start developing when T_0 is increased beyond about 215°C. These results suggest that the design values of T_0 should be around 215°C, to minimize the effect of unforeseen fluctuations in T_0 on product properties.

Figures 10 and 11 show the effect of varying the jacket temperature. Lowering the jacket temperature is seen to have some effect on the profiles

TABLE IV
Product Characteristics for Different Sets of Conditions

Run	Variable changed	Value[a]	Product characteristics: Conversion of C_1 (%)	Product characteristics: $10^2[C_2]$ (mol/kg)	Product characteristics: μ_n
0	$[W]_0$ (mol/kg)	0.15 (reference)	90.87	2.89	174.15
1		0.10	13.73	0.10	40.31
2		0.13	52.90	0.50	99.96
3		0.14	89.82	2.19	180.12
4		0.18	91.02	3.59	156.6
5	T_0 (°C)	210	30.89	0.23	54.88
6		211	41.31	0.33	70.36
7		211.3	45.56	0.39	78.97
8		211.5	88.76	1.87	172.68
9		212	89.11	1.94	173.17
10		213	89.66	2.08	173.85
11		220	90.75	3.65	171.01
12	T_J (°C)	220	36.25	0.28	62.57
13		225	88.80	1.86	173.83
14		230	89.17	1.94	174.19
15		240	90.25	2.26	175.12
16	S (m/m)	10	48.87	0.43	83.03
17		16	90.92	3.32	173.77
18	U_t	3.0	51.11	0.45	87.03
19	(kcal/mol-h-K)	4.0	81.38	1.22	156.31
20		4.5	89.48	2.05	172.67
21		5.5	90.91	3.43	173.61
22	$V_{t,0}$ (m/s)	180	90.95	3.75	173.80
23		210	88.99	1.95	171.68
24	r_t (m)	0.024	90.99	3.43	174.43
25		0.026	88.99	1.82	169.95
26		0.027	28.83	0.21	52.15
27	r_c (m)	0.32	24.79	0.18	46.63
28		0.38	91.08	3.51	175.33
29	L (m)	18	41.43	0.34	70.66
30		22	90.96	3.70	173.84

[a]All other variables at their reference values.

$T(x)$ and $\mu_n(x)$, although the values at the exit of the reactor are almost unaffected until $T_J = 220$°C. It must be emphasized that the latter conclusion stems from the fact that the length of the reactor being studied ensures near-equilibrium product conditions, and that, if L were shorter, significant differences in the product properties would be obtained. Lowering T_J leads to a general cooling down of the reaction mass over most of the length of the reactor. However, results are found to become sensitive to T_J and the reaction starts getting quenched when this variable is taken below about 225°C. The

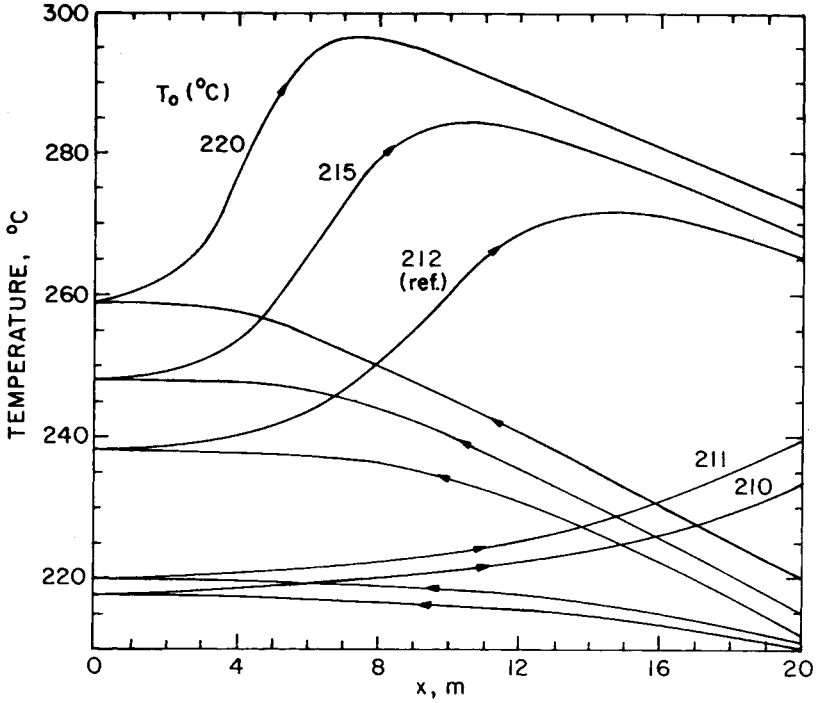

Fig. 8. Effect of the feed temperature T_0 on the temperature profile in the reactor.

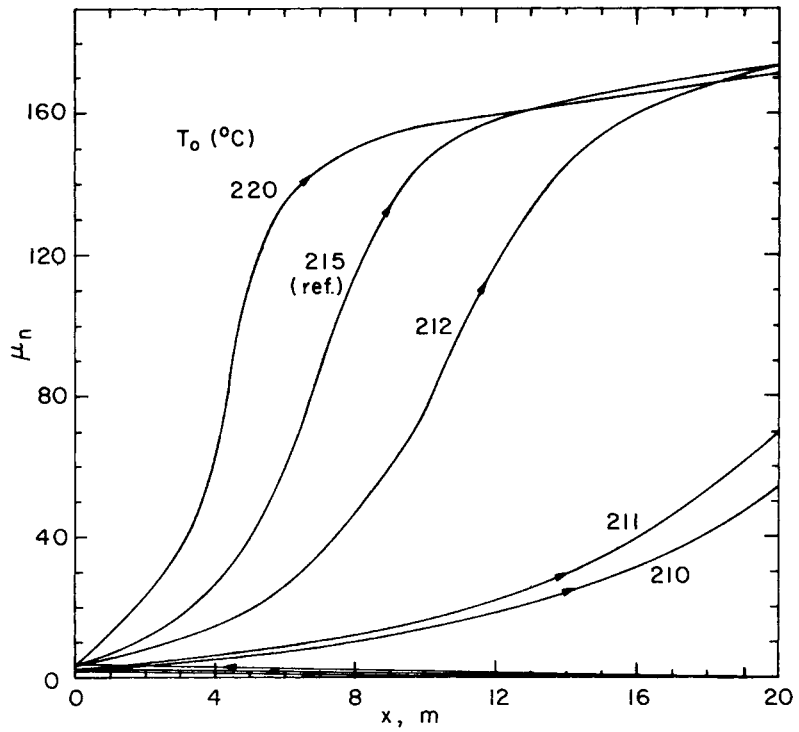

Fig. 9. Effect of T_0 on $\mu_n(x)$.

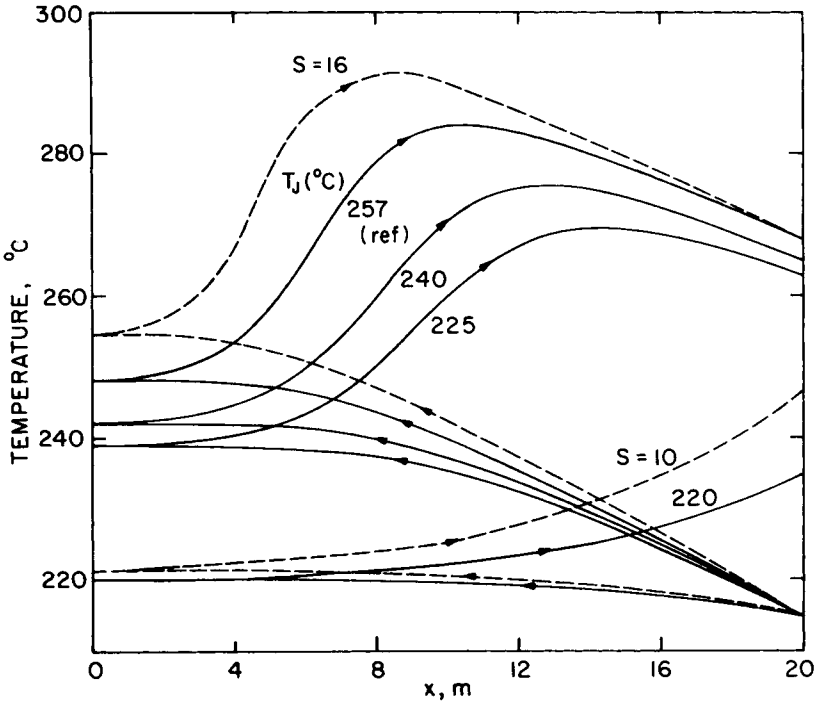

Fig. 10. Effect of U_J (solid) and S (dotted) on $T(x)$.

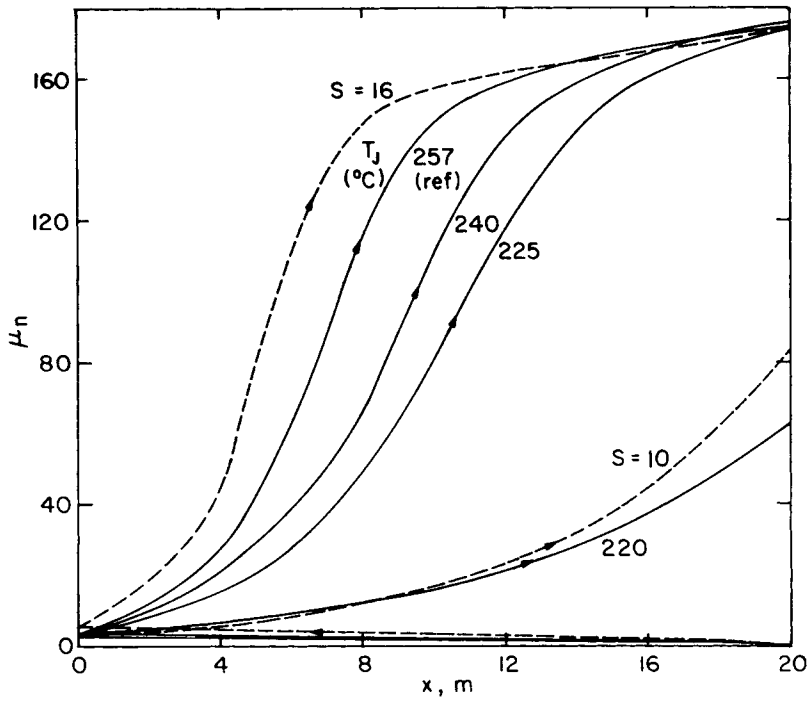

Fig. 11. Effect of U_J (solid) and S (dotted) on $\mu_n(x)$.

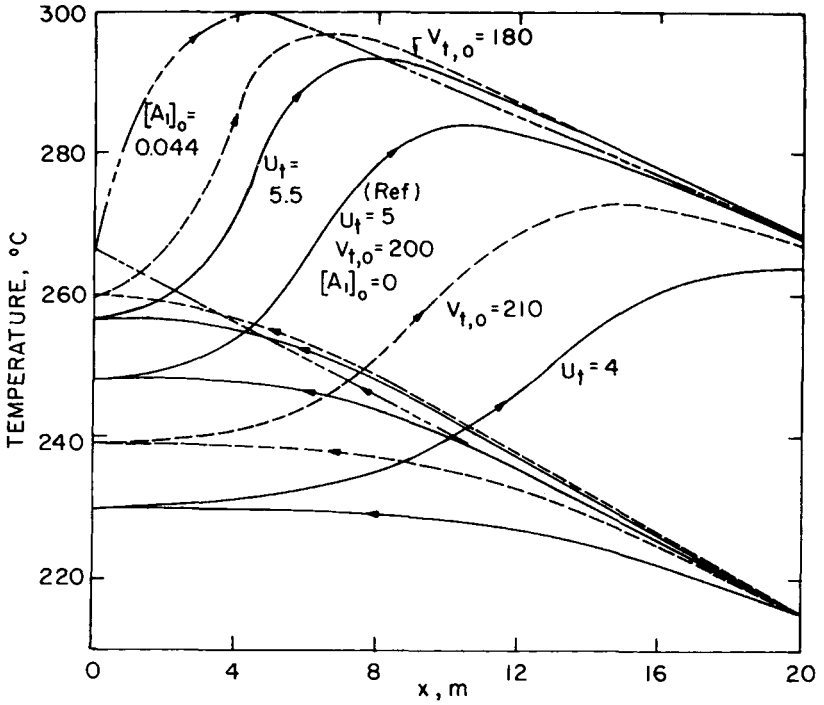

Fig. 12. Effect of U_t (solid), $V_{t,0}$ (dotted), and $[A_1]_0$ (----) on $T(x)$. Reference run has $U_t = 0$, $V_{t,0} = 200$, and $[A_1]_0 = 0$. Units for the various quantities are as specified in Nomenclature.

relative insensitivity of results to U_J and T_J are thus limited only to a certain range of values. A comparison of Figures 10 and 2 (for $U_J = 0$ and $U_t = 5$) reveals that it is more fruitful to insulate the reactor, at times, than to use a jacket fluid having too low a temperature. Figures 10 and 11 also show the effect of S, the parameter characterizing the degree of coiling on the tube side. An increase in S leads to a small increase in the residence times of the reaction mass. What is more important, however, is that the heat transfer characteristics of the system change. Increasing S from the reference value of 15 to 16 leads to a considerable preheating of the reaction mass inside the tube, and the temperature peak becomes more acute. Lowering S to 10 almost quenches the reaction. Table IV (runs 0, 16, and 17) shows that the product characteristics for $S = 15$ and 16 do not differ significantly.

The effects of U_t, $V_{t,0}$ and $[A_1]_0$ are shown in Figures 12 and 13. The trends are as expected intuitively. An increase in U_t leads to a significant preheating of the reaction mass inside the tube and so leads to a temperature peak in the column. Lower values of Δx are required to obtain numerically stable solutions. In fact, results for $U_t = 5.5$ kcal/m^2-h-K required a Δx of 0.025 m. The sensitivity of the profiles to U_t must be noted. A higher value of U_t than 5.5 kcal/m^2-h-K would lead to much higher temperatures and is of little practical importance because of the possibility of degradation reactions. Results for different feed rates $V_{t,0}$ are shown in Figures 12 and 13. The values of U_t and U_J have been kept at their reference values, even though they may change because of a change in the Reynolds number associated with $V_{t,0}$. A lower $V_{t,0}$ leads to an increase in the residence times in the tube and so to an increase in preheating and to higher temperature peaks in the column. The addition of

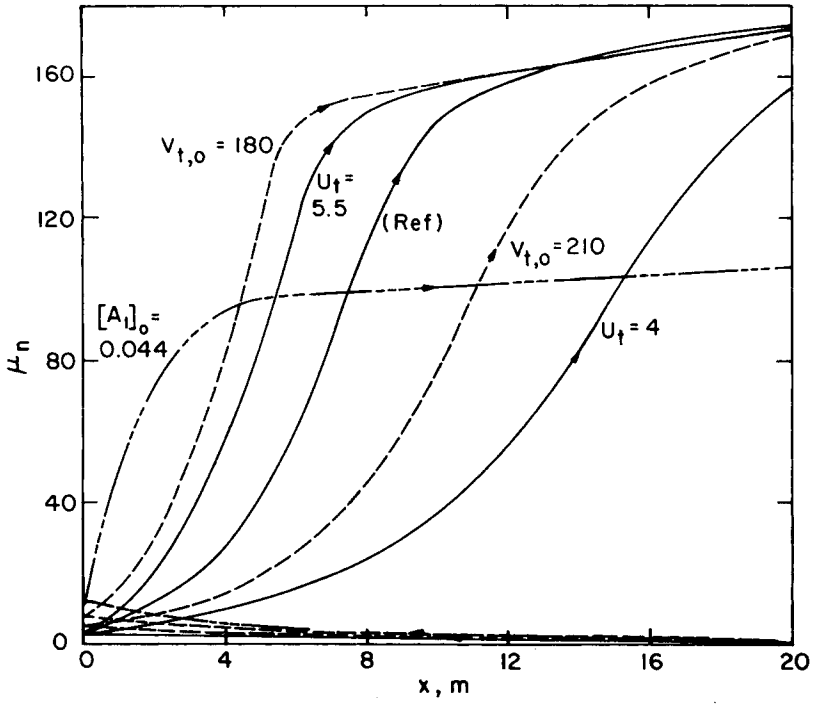

Fig. 13. Effect of U_t (solid), $V_{t,0}$ (dotted); and $[A_1]_0$ (----) on $\mu_n(x)$. Conditions as in Figure 12.

monofunctional acid A_1 in the feed leads to lower values of μ_n. However, the addition of A_1 leads to higher initial reaction rates, which explains the very high temperature peaks in Figure 12. One must ensure that the addition of monofunctional acid does not lead to too high a temperature peak in the column (which can lead to degradation of the polymer).

Figures 14 and 15 show the effects of some other reactor dimensions, namely, r_t, r_c, and L. Reference values for U_t and U_J have been used, even though a change in the reactor dimensions may lead to changes in the values of the heat transfer coefficients (we have followed this approach since we are only interested in the sensitivity of the results to different parameters). Table IV gives results for some other conditions. It is observed that reducing L quenches the reaction (run 29, Table IV) because of the shorter residence time and so reduced preheating in the tube. Similarly, increasing the radius of the column r_c (with $V_{t,0}$ at the reference value) leads to more heat generated and so to higher temperatures. An increase in r_t, with $v_{t,0}$ unchanged, leads to two opposing effects—the possibility of increased preheating of the reaction mass in the tube and the significant reduction in the residence time in the column (since more material is now flowing in the same size of column). The results in Figures 14 and 15 indicate that the latter effect predominates and a partial quenching of the reaction is observed.

It may be mentioned that, in several of our simulation runs, the temperatures in the tube near the feed end are below about 220°C and the rate constants used may not be correct. This does not lead to any serious errors, since in this zone negligible polymerization takes place and the temperature rises primarily because of heat transfer from the column side. Our simulation

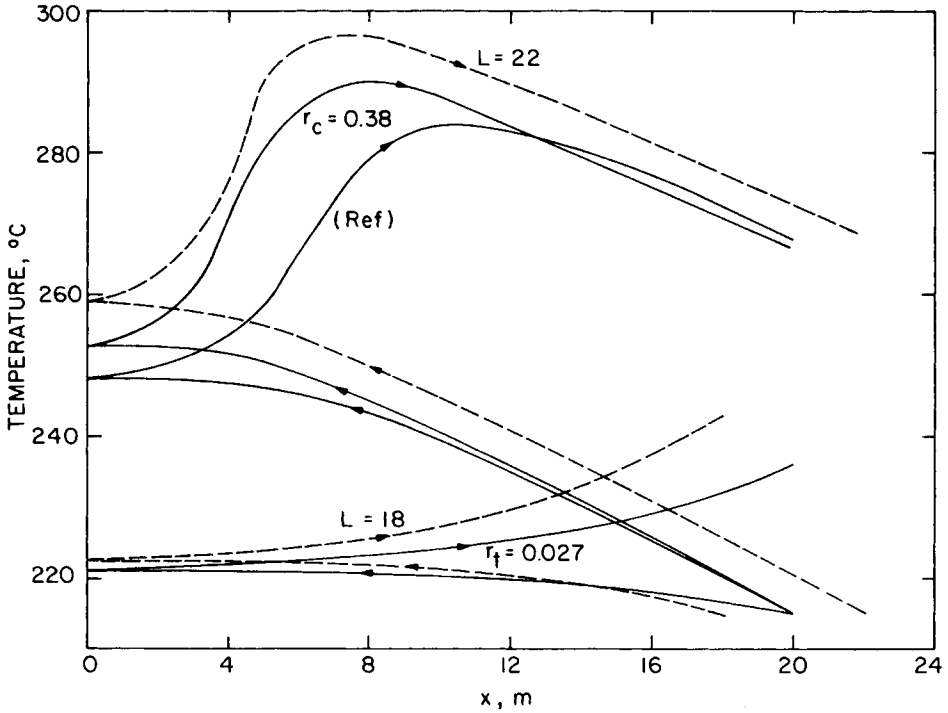

Fig. 14. Effect of r_t, r_c, and L on $T(x)$. Reference run has $L = 20$ m, $r_c = 0.35$ m, and $r_t = 0.025$ m.

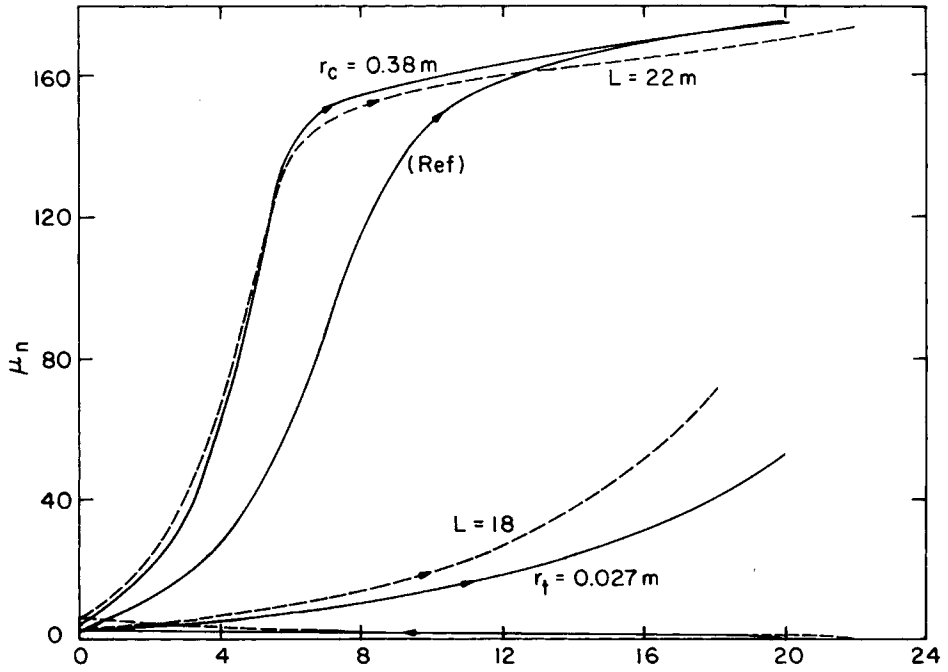

Fig. 15. Effect of r_t, r_c, and L on $\mu_n(x)$. Conditions as in Figure 15.

results (with slightly different parameter values) have been found to be consistent with some industrial data on a nylon 6 reactor, but details of these comparisons cannot be provided for proprietary reasons. The various approximations used are therefore justified, and our model is appropriate for designing digital-control systems.

CONCLUSIONS

An industrial nylon 6 reactor that is energy integrated has been simulated. The steady-state model presented is simple enough that it can be used to design digital-control algorithms. Yet, the model accounts for all the important features. A sensitivity study has been carried out using this model, and it is observed that there is a temperature maximum in the column under usual operating conditions. This peak is quite sensitive to minor changes in the feed conditions and could, at times, lead to undesirable product characteristics because of degradation reactions set off at high temperatures. Under certain conditions, e.g., those shown in Figure 7, this model suggests the presence of interesting dynamic (unsteady) features in the operation of such reactors.

NOMENCLATURE

A_i, A_i^c	Frequency factor of ith reaction (uncatalyzed and catalyzed), kg/mol-h or kg^2/mol^2-h
A	Cross-sectional area, m^2
C_p	Specific heat of reaction mass, kcal/kg-K
E_i, E_i^c	Activation energy of ith reaction, cal/mol
$\Delta H_{r,i}$	Heat of ith reaction, cal/mol
ΔH_i	Enthalpy of ith reaction, cal/mol
K_i	Equilibrium constant
k_i, k_i'	Rate constants for forward and reverse reactions, kg/mol-h
L	Length of reactor, m
R	Gas constant, cal/mol-K
$\mathcal{R}_i$	Net forward rate of ith reaction, mol/kg-h
r	Inner radius, m
S	Actual length of tube in 1 m of column length, m/m
ΔS_i	Entropy of ith reaction, cal/mol-K
T	Temperature, K
U	Overall heat transfer coefficient, kcal/m^2-h-K
V	Velocity, m/h
x	Position from top of reactor, m

Greek Letters

μ_k, μ_k'	kth moments of bifunctional and monofunctional species, mol/kg
ρ	Density of reaction mass, kg/m^3
ξ_i	Concentrations or moments (Table II), mol/kg

Superscript

(k)	kth iteration

Subscripts

c	Column side
J	Jacket

0 Feed values
t Tube side

Symbols

[ ] Concentrations, mol/kg
$\dot{\xi}_i$ Rate of production of ξ_i

References

1. M. Sittig, *Polyamide Fiber Manufacture*, Noyes Data Corp., Park Ridge, New Jersey, 1972.
2. H. K. Reimschuessel, *J. Polym. Sci., Macromol. Rev.*, **12**, 65 (1977).
3. K. Tai and T. Tagawa, *Ind. Eng. Chem., Prod. Res. Dev.*, **22**, 192 (1983).
4. S. K. Gupta and A. Kumar, *J. Macromol Sci., Rev. Macromol Chem. Phys.*, **C26**, 183 (1986).
5. S. K. Gupta and A. Kumar, *Reaction Engineering of Step Growth Polymerization*, Plenum Press, New York, 1987.
6. H. Jacobs and C. Schweigman, Proceedings of V European/II International Symposium on Chemical Reaction Engineering, Amsterdam, May 2–4, 1972.
7. W. F. H. Naudin ten Cate, Proceedings of International Congress on Use of Electronic Computers in Chemical Engineering, Paris, April 1973.
8. A. Gupta and K. S. Gandhi, *Ind. Eng. Chem., Prod. Res. Dev.*, **24**, 327 (1985).
9. K. Tai, H. Teranishi, Y. Arai, and T. Tagawa, *J. Appl. Polym. Sci.*, **24**, 211 (1979).
10. K. Tai, H. Teranishi, Y. Arai, and T. Tagawa, *J. Appl. Polym. Sci.*, **25**, 77 (1980).
11. K. Tai, Y. Arai, H. Teranishi, and T. Tagawa, *J. Appl. Polym. Sci.*, **25**, 1789 (1980).
12. Y. Arai, K. Tai, H. Teranishi, and T. Tagawa, *Polymer*, **22**, 273 (1981).
13. K. Tai, Y. Arai, and T. Tagawa, *J. Appl. Polym. Sci.*, **27**, 731 (1982).
14. K. Tai and T. Tagawa, *J. Appl. Polym. Sci.*, **27**, 2791 (1982).
15. S. K. Gupta, and A. Kumar, and K. K. Agarwal, *J. Appl. Polym. Sci.*, **27**, 3089 (1982).
16. S. K. Gupta, D. Kunzru, A. Kumar, and K. K. Agarwal, *J. Appl. Polym. Sci.*, **28**, 1625 (1983).
17. A. Ramagopal, A. Kumar, and S. K. Gupta, *Polym. Eng. Sci.*, **22**, 849 (1982).
18. K. Tai, Y. Arai, and T. Tagawa, *J. Appl. Polym. Sci.*, **28**, 2527 (1983).
19. S. K. Gupta, B. S. Damania, and A. Kumar, *J. Appl. Polym. Sci.*, **29**, 2177 (1984).
20. A. Ramagopal, A. Kumar, and S. K. Gupta, *J. Appl. Polym. Sci.*, **28**, 2261 (1983).
21. A. K. Ray and S. K. Gupta, *Polym. Eng. Sci.*, **26**, 1033 (1986).
22. A. K. Ray and S. K. Gupta, *J. Appl. Polym. Sci.*, **30**, 4529 (1986).
23. B. A. Finlayson, *Nonlinear Analysis in Chemical Engineering*, McGraw-Hill, New York, 1980.
24. P. H. Hermans, D. Heikens, and P. F. van Velden, *J. Polym. Sci.*, **30**, 81 (1958).
25. P. J. Hoftyzer, J. Hoogschagen, and D. W. van Krevelen, *Chem. Eng. Sci.*, **20**, 247 (1965).
26. M. Cave, M.S. Dissertation, Imperial College, London, 1975.
27. S. K. Gupta, A. Kumar, P. Tandon, and C. D. Naik, *Polymer*, **22**, 481 (1981).
28. S. K. Gupta, C. D. Naik, P. Tandon, and A. Kumar, *J. Appl. Polym. Sci.*, **26**, 2153 (1981).
29. H. M. Hulburt and S. Katz, *Chem. Eng. Sci.*, **19**, 555 (1964).
30. O. Levenspiel, *Engineering Flow and Heat Exchange*, Plenum Press, New York, 1984.
31. R. A. Mashelkar, *Chem. Ind. Dev.*, **10(9)**, 17 (1976).

Received May 19, 1986
Accepted June 2, 1986